Revision 2

Dependence of R fluorescence lines of rubies on Cr^{3+} concentration at various temperatures

Gao Rong[1, 2, *], Li Heping[1, #], Zhao Jingtai[2, 3]

[1]Key Laboratory of High-temperature and High-pressure Study of the Earth's Interior, Institute of Geochemistry, Chinese Academy of Sciences, Guiyang, Guizhou Province, 550002, P. R. China

[2]Key Laboratory of Transparent Opto-Functional Inorganic Materials, Shanghai Institute of Ceramics, Chinese Academy of Sciences, Shanghai 200050, P. R. China

[3]School of Materials Science and Engineering, Shanghai University, Shanghai 200072, P. R. China

* Now at Shanghai Institute of Ceramics, Chinese Academy of Sciences

[#] E-mail: liheping@vip.gyig.ac.cn

Abstract

The R fluorescence lines of rubies that contain 0.022, 0.068, 0.211, 0.279, 0.556, 1.221 and 1.676 wt% of Cr_2O_3 were measured at temperatures of 100-600 K and at atmospheric pressure. The R_1 line wavenumbers of all of the ruby samples shifted

linearly as the temperature increased from 298 to 600 K at atmospheric pressure, and the temperature dependence increased from -0.157 ± 0.001 cm^{-1}/K to -0.149 ± 0.001 cm^{-1}/K as the Cr_2O_3 content in the rubies increased from 0.022 wt% to 1.676 wt%, which suggests a significant dependence on Cr^{3+} concentration. At room temperature and atmospheric pressure, the full width at half maximum (*FWHM*) of the peak height of the R lines also appears to be linearly related to the Cr^{3+} concentration. The relative intensity ratios of the R_2 to R_1 lines (I_2/I_1) of ruby samples with different Cr^{3+} concentrations show several non-linear variations with temperature from 100 to 600 K, and the maximum values, $(I_2/I_1)_{max}$, occur near room temperature. The effect of Cr^{3+} doping on the temperature dependence of the R line wavenumbers should be considered when rubies are used to calibrate the pressure or temperature in high-pressure and high-temperature experiments.

Keywords: R fluorescence lines; pressure calibration; temperature correction; ruby; Cr_2O_3 content

Introduction

Rubies are important photonic crystals, and their R fluorescence lines vary with pressure and temperature. The variations of the wavenumbers of R lines with pressure are commonly used to calibrate the pressure in diamond anvil cells (DACs) (Forman et al. 1972; Mao et al. 1986). The variations in the intensity of R lines have also been used to calibrate temperature in scientific research (Weinstein 1986). Because the R lines are caused by the excitation of the 3d electrons in their ground states and their

subsequent de-excitation from their excitation states and because there are inevitable interactions between Cr^{3+} in the ruby lattice, the concentration of Cr^{3+} in rubies may affect both the pressure and temperature dependence of the R lines at high temperature and high pressure conditions. Therefore, the quantitative investigation of the effect of Cr^{3+} doping on the pressure and temperature behaviors of R lines is important for the accuracy of pressure and temperature calibrations in simultaneous high pressure and high temperature DAC experiments, which are often used to study the Earth's interior (Chou 2003) and in other high-pressure sciences, such as high-pressure physics, chemistry, life science and material science.

Variations in the peak position and the width and intensity of the ruby R_1 line as a function of temperature have been analyzed in several studies, but the results vary widely (Kokhanenko and Antipov 1969; Barnett et al. 1973; Yamaoka et al. 1980; Wunder and Schoen 1981; Ragan et al. 1992; Yen and Nicol 1992; Goncharov et al. 2005). For example, Ragan et al. (1992) determined a temperature dependence of 0.158 cm^{-1}/K from 390-600 K for the R_1 line wavenumber, which was approximately 11% greater than the value of 0.0068 nm/K (equivalent to approximately 0.141 cm^{-1}/K) that was reported by Barnett et al. (1973) and Yamaoka et al. (1980). When calibrating the pressure or temperature in a heating DAC experiment from 300 to 600 K using the R_1 line, this difference would lead to a maximum temperature discrepancy of 34 K or a maximum pressure discrepancy of 675 MPa. In fact, the reference contents of Cr_2O_3 in rubies used by previous researchers (0.062 wt%, 0.5 wt%, ~1 wt%, and 2 wt% Cr_2O_3 by Yen and Nicol 1992; Barnett et al. 1973; Yamaoka et al.

1980; and Wunder and Schoen 1981, respectively) were not the same. Does the concentration of Cr^{3+} contribute to this discrepancy? This study attempts to answer this question by measuring the temperature variations of the R lines of rubies with varying Cr^{3+} concentrations at atmospheric pressure.

Experimental methods

Pink to blood red synthetic rubies were cut into disks that were ~0.5 mm in diameter and ~0.2 mm thick and then polished. The concentrations of Cr^{3+} in the rubies were measured using an EPMA-1600 type electron probe (beam size 10 μm) with WDS (wavelength-dispersive spectroscopy) mode and an Atomic Absorption Spectrophotometer (AAS). Three to five spots were measured in each sample. The average values are listed in Table 1. The Cr_2O_3 contents in rubies were from 0.022 to 1.676 wt%.

In the fluorescence measurement experiments that were conducted at high temperatures and atmospheric pressure, the samples were heated and cooled in a Linkam heating stage with a liquid nitrogen flowing system. The temperature was increased by 15 K/min and measured with a thermocouple. The precision of the temperature measurements was ± 0.1 K. The fluorescence spectra of the samples were excited and recorded using a con-focal Renishaw inVia Micro-Raman Spectroscopy system. The system uses a 514.5 nm laser beam, which is produced by a Spectra Physics 2017 2 W argon ion laser and is focused on a spot on the sample by a Leica microscope system, as the excitation light source of the fluorescence. A

high-resolution white light image of the samples that covers the sampling spot can be displayed on a screen of the Leica microscope system. In our experiments, (1) the silicon 520 cm^{-1} peak calibration was performed before the fluorescence spectra were collected, and the accuracy of the spectrum collection was up to ± 0.01 cm^{-1}; (2) the excitation laser powers ranged from 0.0002 mW to 0.05 mW; (3) a 20X Olympus ULWD objective was used for the Leica microscope system, so the excitation laser beam was focused onto a ~2-μm-diameter spot; and (4) all of the fluorescence spectra were collected near the spots where the electron microprobe measurements were made.

In the fluorescence measurement experiments that were conducted at high pressures and room temperature, the fluorescence spectra of each ruby sample were measured at pressures of 0-2.0 GPa using the fluorescence measurement system described above and a DAC. The anvil culets of the DAC were approximately 500 μm in diameter. The T301 stainless steel gasket (300 μm thick with a sample hole that was 280 μm in diameter) and a mixture of methanol, ethanol and water at 16:3:1 volume proportions were used as the sample chamber and pressure medium, respectively, and could maintain a hydrostatic pressures up to ~10.5 GPa at room temperature (Angel et al. 2007). The pressures in the cell were measured using the wavenumber shift of the R_1 fluorescence peak of ruby #5, which contained 0.556 wt% of Cr_2O_3. The uncertainty of this technique below 2.0 GPa was estimated to be ± 50 MPa (Schmidt and Ziemann 2000).

The wavenumber of each fluorescence peak was obtained using the peak fitting program of the WIRE 3.1 software package from Renishaw Co. The R_1 line generally had a Lorentzian-type shape, but the R_2 line at high temperature was fit better by a Voigt type line that included Gaussian and Lorentzian components, and the Gaussian proportion increased with increasing temperature and Cr^{3+} concentration in the ruby samples.

Finally, the electron densities of state (DOS) of the Cr^{3+} 3d band in the rubies at ambient pressure and 10 GPa were calculated by the first principle calculation method using the crystal structure data of $Al_{1.98}Cr_{0.02}O_3$, $Al_{1.92}Cr_{0.08}O_3$, $Al_{1.896}Cr_{0.104}O_3$ and $Al_{1.54}Cr_{0.46}O_3$ in the ICSD database. The calculations used the Generalized Gradient Approximation (GGA) method, the PBE exchange-correlation function (Perdew et al. 1996) and ultra-soft potentials, and a 3×3×3 *k*-point mesh and 300 eV cut-off energy were chosen.

Results and discussions

1. Fluorescence peaks and their positions

The fluorescence spectra and the Raman spectra of the ruby samples with the lowest and highest Cr_2O_3 contents used in this study are shown in Figure 1. In addition to the well-known R_1 and R_2 peaks, several new peaks were present in the fluorescence spectra of rubies with Cr^{3+} concentrations greater than 0.5 wt%, and the relative intensities of the new peaks increased with increasing Cr_2O_3 content. A high Cr^{3+} concentration would lead to strong Cr^{3+}-Cr^{3+} interactions, which change the electron

structure of the Cr^{3+}. Thus, the new peaks might be attributed to Cr^{3+}-Cr^{3+} interactions in the ruby lattice because the fluorescence spectra of rubies originate from the excitation of the 3d electrons in their ground states and their subsequent de-excitation from their respective excitation states. However, because the Raman spectra were similar, the increase of Cr^{3+} concentration likely does not cause the separation of a new phase from the ruby matrix.

Significantly varying shifts of the wavenumber positions of the R lines with Cr^{3+} concentration were observed at room temperature and atmospheric pressure. As shown in Figures 2a and 2b, the wavenumbers of the R_1 and R_2 lines decreased with increasing Cr_2O_3 content up to 0.3 wt%, whereas a reversal of this trend occurred at Cr_2O_3 contents greater than 0.3 wt%. The latter observation might be attributed to the fact that the ionic radius of Cr^{3+} is larger than that of Al^{3+}. The behavior at Cr_2O_3 contents below approximately 0.3 wt% is not fully understood, but it might be related to the internal stress that commonly remains in ruby samples because we did not attempt to eliminate the residual stress in our samples before making the fluorescence measurements.

From 300 to 600 K and at atmospheric pressure, the R lines red-shifted linearly with increasing temperature. The relationship between the slope of the R_1 shift with temperature and Cr_2O_3 content is shown in Figure 3a. The absolute values of the slopes decrease with increasing Cr_2O_3 content. The corresponding relationship for R_2 is shown in Figure 3b. In this case, the absolute values of the slopes of the wavenumber shift with temperature also decrease with increasing Cr_2O_3 content

153 below 1.2 wt% content of Cr_2O_3 but recover at higher contents.

154 Rangan et al. (1992) observed slopes of the R_1 and R_2 shifts with temperature of
155 -0.158 cm^{-1}/K and -0.162 cm^{-1}/K from 300-600 K, respectively, with an unknown Cr^{3+}
156 concentration. They attributed the discrepancy between their results and those of other
157 researchers (-0.14 cm^{-1}/K for R_1 measured by Barnett et al. 1973; -0.153 cm^{-1}/K for
158 R_1 by Yen and Nicol 1992) to the different methods used to determine the peak
159 positions in the spectra fitting. Spectrum fitting to a double Lorentzian line can allow
160 us to accurately separate the R_1 and R_2 components from overlapping R lines and
161 thereby obtain precise line positions, while obtaining the peak positions by eye (as in
162 Barnett et al. 1973 and Yen and Nicol 1992) will give a R_1 position that does not shift
163 as fast as it should because at high temperatures, the R_1 and R_2 lines overlap and yield
164 a visual R_1 peak that is located at a higher frequency than the line's true resonant
165 frequency. However, significant differences are still present in the slopes of the R line
166 shift among the samples in this study (see Table 2 and Figures 3 (a) and (b)) even
167 though the wavenumber positions of the R lines were obtained by fitting the spectrum
168 to a double Lorentzian line using high-precision software. Therefore, the
169 discrepancies in the slopes of the R line shift with temperature between various
170 studies cannot be fully explained by the difference in the methods of determining the
171 peak positions. We believe that the major factor was the difference in the Cr^{3+}
172 concentrations in the ruby samples used in this study. The mechanism is discussed in a
173 subsequent section. The anomalous slope of R_2 in sample #1006 and #8 might be
174 attributed to the crystal orientation (Shen and Gupta 1993). The relative intensity of

175 R_1 and R_2 can reflect the crystal orientations in the rubies to some extent. The shifts of
176 the slopes of the R_2 lines with temperature were more closely related to the intensity
177 ratios of R_2 and R_1 (I_2/I_1) (see Figures 3c and 3d), which is consistent with the greater
178 dependence on the crystal orientation of the R_2 line shift than the R_1 line shift (Shen
179 and Gupta 1993). Moreover, of all the samples, sample #1006 and #8 had the higher
180 I_2/I_1 value (Table 2). In sample #1006 and #8, the fast shift of the R_2 line indicates that
181 the crystal orientation might be closer to the crystal's c axis. However, the anomalous
182 fast shift of the R_1 line in sample #1006 might be attributed to the lower Cr^{3+}
183 concentration, the crystal orientation and the internal stress.
184 In the high pressure DAC experiments (0-2.0 GPa), we found no significant pressure
185 difference in the cell when we used the ruby samples with different Cr_2O_3 contents as
186 pressure calibrants. Figure 4 shows the differences between the pressure that was
187 measured using sample #5 and used as the reference pressure in our high pressure
188 experiments and the pressures measured using the other ruby samples with different
189 Cr_2O_3 contents. All of the differences between the reference pressure and the other
190 measured pressures are within ± 50 MPa, which is a commonly-used uncertainty for
191 pressure calibrations when rubies are used as a pressure calibrant in hydrostatic DACs
192 below 2 GPa (Schmidt and Ziemann 2000).

193 **2. Additional discussion of the impact of Cr^{3+} concentration on the R line shift**

194 Temperature and pressure both have significant impacts on the red-shift of R
195 lines due to the Cr^{3+} doping in rubies. In this study, we found that the Cr^{3+}
196 concentration in a ruby also has an important impact on shift of the R lines. This

impact can be summarized as a decrease of the ($d\nu/dT$) value of the R lines and a blue-shifting of the R lines with increasing Cr^{3+} concentration in a ruby.

McCumber and Sturge (1963) theoretically interpreted the shift of the R_1 line with temperature. Based on Equation (3a) of McCumber and Sturge, we calculated the derivative of the wavenumber of the R_1 line with respect to temperature as follows,

$$\frac{d\nu_1(T)}{dT} = a \cdot [4 \times \frac{T^3}{T_D} \int_0^{T_D/T} dx \frac{x^3}{e^x - 1} - \frac{1}{T(e^{T_D/T} - 1)^2}] \quad (1),$$

where a is the electron-phonon coupling constant, and T_D is the effective Debye temperature. McCumber and Sturge (1963) found that using a = -400 cm^{-1} and T_D = 760 K provided a good fit to the experimental results for 0-700 K. However, Yen and Nicol (1992) found that a = 400 cm^{-1} gives good results for this temperature range. Table 3 shows the values of the constant a that provided the best fits to the measurement results in this study. The rates of the wavenumber shift of the R lines with temperature are closely related to the electron-phonon coupling constant, and the electron-phonon coupling constant a decreases monotonously with increasing Cr^{3+} concentration. According to McCumber and Sturge (1963), the electron-phonon coupling constant a measures the probability of the scattering of phonons from the 3d electrons of Cr^{3+}; the larger the value of a, the smaller the probability of scattering. In our case, an increase of the Cr^{3+} concentration in the ruby samples indicates an increase of the density of the scattering center, Cr^{3+}, for the phonon. As a result, the probability of scattering would increase, and the value of the phonon-electron coupling constant a decreases with increasing Cr^{3+} concentration. Therefore, our experimental results are consistent with the theoretical model of McCumber and

Sturge (1963) of the impact of Cr^{3+} concentration on the value of ($d\nu/dT$) of R lines. To theoretically explain the blue-shift of ruby R lines with increasing Cr^{3+} concentration, we used the first principle calculation method and conducted a series of calculations of the electronic density of state (DOS) of the Cr^{3+} 3d band for rubies with different Cr^{3+} concentrations at room temperature and atmospheric pressure and at room temperature and 10 GPa. The results (Figures 5 and 6) show that the peaks of the DOS of the Cr^{3+} 3d electrons are blue-shifted with increasing Cr^{3+} concentration at room temperature and atmospheric pressure and red-shifted with increasing pressure at room temperature and a constant Cr^{3+} concentration. Moreover, with increasing Cr^{3+} concentration at room temperature, the amplitude of the pressure-induced red-shift of the DOS peaks increased when the pressure increased from atmospheric pressure to 10 GPa. Because the red-shift of the DOS peaks of the Cr^{3+} 3d electrons with increasing pressure is a well-known mechanism for the red-shift of ruby R lines with pressure (Xie 2004), the blue-shift of the DOS peaks of the Cr^{3+} 3d electrons with increasing Cr^{3+} concentration should also be the mechanism for the blue-shift of the ruby R lines with increasing Cr^{3+} concentration. This behavior was observed from the experimental results in this study.

The analysis presented above indicates that the Cr^{3+} concentration might have a significant influence on the R line shift of rubies in addition to the important factors of temperature and pressure. It is possible that with increasing Cr^{3+} concentration, there could be increasingly important coupling effects of the influences of temperature, pressure and Cr^{3+} concentration on the ruby R line shift because the Cr^{3+}- Cr^{3+}

241 interactions in the ruby lattice would become stronger (Ohnishi and Sugano 1982;
242 Winter et al. 1990).

243 **3. Full width at half maximum (*FWHM*) of the R lines**

244 The full width at half maximum of the R_1 line ($FWHM_1$) at atmospheric pressure and
245 temperature increased significantly with increasing Cr^{3+} concentration, whereas the
246 full width at half maximum of the R_2 line ($FWHM_2$) increased moderately (Figure 7).
247 By linear fits to the experimental data for the R_1 and R_2 lines, we obtained $FWHM_1$
248 (cm^{-1}) = 11.44348 + 2.33563 × Cr_2O_3 (wt%) with a r^2 value of 0.9978 and $FWHM_2$
249 (cm^{-1}) = 8.94403 + 1.1267 × Cr_2O_3 (wt%) with a r^2 value of 0.9986. In contrast,
250 Ragan et al. (1992) reported that the *FWHM* values of the R lines of rubies that
251 contained 0.12% and 0.5% Cr^{3+} were nearly identical. Theoretically, if two 3d
252 electrons are located in the same type of orbit but belong to two different Cr^{3+} in the
253 ruby lattice, there is always a slight difference in their energy levels due to subtle
254 differences in the electromagnetic environments in which the two Cr^{3+} are located.
255 The difference in energy level changes the energy level into an energy band. With
256 increasing Cr^{3+} concentration in rubies, the energy bands of both the ground states and
257 the excited states of the 3d electrons of Cr^{3+} would widen, and the *FWHM*s of the
258 ruby R lines that originate from the excitation of 3d electrons from their respective
259 ground states and the subsequent de-excitation from their corresponding excitation
260 states of Cr^{3+} would also widen. As shown in Figure 7, both $FWHM_1$ and $FWHM_2$
261 show significant linear increases with Cr^{3+} concentration in the range of 0.022-1.67
262 wt%. Our experimental results are consistent with the theoretical analysis presented

above.

At high temperatures and ambient pressure, $FWHM_1$ increased with temperature from 298-600 K (Figure 8). These results are consistent with common knowledge. However, two interesting phenomena in our results are worth noting. First, the increasing width of the *FWHM*s of the R lines with increasing Cr^{3+} concentration observed at room temperature (Figure 7) was also observed for the R_1 line at higher temperatures. Second, the positive dependence of $FWHM_1$ on temperature became stronger with increasing temperature.

4. Relative intensity ratios of R_2 to R_1 (I_2/I_1)

Similar to the results described above, the relative intensities of the R_1 and R_2 lines of all of the ruby samples in this study decreased with increasing temperature at atmospheric pressure. However, the relative intensity of the R_2 line (I_2) decreased more slowly than that of the R_1 line (I_1) at temperatures from 100 K to approximately 298 K and subsequently decreased faster than I_1 until 600 K, which indicates a significant temperature dependence of I_2/I_1 (Figure 9a in the supplement information). Moreover, the maximum I_2/I_1 values, $(I_2/I_1)_{max}$, occurred at different temperatures in samples with different Cr_2O_3 contents, and the values of $(I_2/I_1)_{max}$ and I_2/I_1 at 298 K, i.e., $(I_2/I_1)_0$, were both related to the Cr_2O_3 contents in the samples. As shown in Figure 9b in the supplement information, the temperatures that correspond to the values of $(I_2/I_1)_{max}$ were inversely related to the Cr_2O_3 content. However, it is interesting to note that the relationship between $(I_2/I_1)_{max}$ and the Cr_2O_3 content was weaker than that between $(I_2/I_1)_0$ and the Cr_2O_3 content at atmospheric pressure. By

285 further linear fitting, we obtained a relationship between $(I_2/I_1)_{max}$ and $(I_2/I_1)_0$, which
286 can be expressed as $(I_2/I_1)_{max} = -0.02036 + 1.04067 \times (I_2/I_1)_0$ with a r^2 value of 0.997
287 (Figure 9c in the supplement information).
288

289 ## Implications

290 Pressure calibration is of primary importance for high pressure experiments. Ruby is
291 the most commonly used pressure calibrant, especially in high pressure DAC
292 experiments. Temperature corrections in ruby pressure calibrations are especially
293 important at elevated temperatures. The results of this study show that the
294 wavenumber shifts of ruby R lines are related not only to variations of pressure and
295 temperature but also to variations in the Cr^{3+} concentrations of the rubies. Moreover,
296 the three influential factors, temperature, pressure and Cr^{3+} concentration, have
297 important coupled effects on the wavenumber shifts of the ruby R lines. At room
298 temperature and pressures of 0-2.0 GPa, the results of our DAC experiments show
299 that the differences in the cell pressures calibrated by the ruby samples with different
300 Cr^{3+} concentrations were less than ± 50 MPa, which is a commonly accepted pressure
301 calibration uncertainty for a ruby calibrant in hydrostatic DACs below 2.0 GPa
302 (Schmidt and Ziemann 2000). However, this does not mean that the differences would
303 be within ± 50 MPa at higher temperatures and/or pressures. For example, if we
304 conduct a heating DAC experiment from 300 to 600 K and calibrate the temperature
305 or pressure using the temperature shift rates of the R_1 line wavenumber of samples
306 #1006 and #8 (Table 2), the maximum temperature and pressure differences would be

16 K and 315 MPa, respectively. We conclude that before conducting a DAC experiment, it is important to know the dependence of the ruby R line shift on the temperature, pressure and Cr^{3+} concentration if rubies are used as the temperature or pressure calibrant. The precision of the ruby temperature or pressure calibration could be improved significantly if these dependences are known in detail. However, a large number of experiments at higher pressures and/or temperatures should be conducted in the future to completely resolve the complicated coupled effects of temperature, pressure, and Cr^{3+} concentration on the wavenumber shifts of the R lines of rubies.

References

Angel, R.J., Bujak, M., Zhao, J., Gatta, G.D., and Jacobsen, S.D. (2007) Effective hydrostatic limits of pressure media for high-pressure crystallographic studies. Journal of Applied Crystallography, 40, 26-32.

Barnett, J.D., Block, S., and Piermarini, G.J. (1973) An optical fluorescence system for quantitative pressure measurement in the diamond-anvil cell. Review of Scientific Instruments, 44, 1-9.

Chou, I.M. (2003) Hydrothermal diamond-anvil cell: application to studies of geologic fluids. Acta Petrologica Sinica, 19, 213-220.

Debiasi, R.S. and Rodrigues, D.C.S. (1981) Influence of chromium concentration and particle size on the ESR linewidth of Al_2O_3: Cr^{3+} powders. Journal of Materials Science, 16, 968-972.

Forman, R.A., Piermarini, G.J., Barnett, J.D. and Block, S. (1972) Pressure measurement made by the utilization of ruby sharp-line luminescence. Science, 176, 284-285.

329 Kokhanenko, P.N. and Antipov, A.B. (1969) Possible determination of the emission wavelength of
330 active ruby from its temperature. II. Russian Physics Journal, 12, 37-40.
331 Goncharov, A.F., Zaug, J.M., and Crowhurst, J.C. (2005) Optical calibration of pressure sensors
332 for high pressures and temperatures. Journal of Applied Physics, 97, 094917-094917-5.
333 Goossens, R.J.G., Dijkhuis, J.I. and Wijn, H.W.de. (1985) Relaxation of 29 cm^{-1} phonons in ruby.
334 Physical Review B, 32, 7065-7075.
335 Mao, H.K., Xu, J. and Bell, P.M. (1986) Calibration of the ruby pressure gauge to 800 kbar under
336 quasi-hydrostatic conditions. Journal of Geophysical Research, 91, 4673-4676.
337 McCumber, D.E. and Sturge, M.D. (1963) Linewidth and temperature shift of the R lines in ruby.
338 Journal of Applied Physics, 34, 1682-1684.
339 Ohnishi, S. and Sugano, S. (1982) Theoretical studies of high-pressure effects on optical
340 properties of ruby. Japanese Journal of Applied Physics, 21, L309-L311.
341 Perdew, J.P., Burke, K. and Ernzerhof, M. (1996) Generalized gradient approximation mad simple.
342 Physical Review Letters, 77, 3865-3868.
343 Ragan, D.D., Gustavsen, R. and Schiferl, D. (1992) Calibration of the ruby R_1 and R_2 fluorescence
344 shifts as a function of temperature from 0 to 600K. Journal of Applied Physics, 72,
345 5539-5544.
346 Schmidt, C. and Ziemann, M.A. (2000) In-situ Raman spectroscopy of quartz: A pressure sensor
347 for hydrothermal diamond-anvil cell experiments at elevated temperatures. American
348 Mineralogist, 85, 1725-1734.
349 Shen, X.A. And Gupta, Y.M. (1993) Effect of crystal orientation on ruby R-line shifts under shock
350 compression and tension. Physical Review B, 48, 2929-2940.

Szabo, A. (1971) Observation of the optical analog of the mossbauer effect in ruby. Physical Review Letters, 27, 323-326.

Weinstein, B.A. (1986) Ruby thermometer for cryobaric diamond-anvil cell. Review of Scientific Instruments, 57, 910-913.

Winter, N.W., Ross, M. and Pitzer, R.M. (1990) Calculation of the pressure shifts of the quartet states of ruby. Journal of Physical Chemistry, 94, 1172-1174.

Wunder, S.L. and Schoen, P.E. (1981) Pressure measurement at high temperatures in the diamond anvil cell. Journal of Applied Physics, 52, 3772-3775.

Xie, Y.L. (2004) High temperature high pressure study of the R1 ruby fluorescence line, 41-46 p. Master. thesis, Jilin University, Changchun.

Yamaoka, S., Shimomura, O. and Fukunaga, O. (1980) Simultaneous measurements of temperature and pressure by the ruby fluorescence line. Proceedings of the Japan Academy. Ser. B: Physical and Biological Sciences, 56, 103-107.

Yen, J. and Nicol, M. (1992) Temperature dependence of the ruby luminescence method for masuring high pressure. Journal of Applied Physics, 72, 5535-5538.

Tables

Table 1. Weight percentages of major and trace elements in the ruby samples.

Sample No.	1006	4	3	2	5	7	8
Cr_2O_3	0.022*	0.068	0.211	0.279	0.556	1.221	1.676
Fe_2O_3	-	0.002	0.001	0.002	0.011	0.024	0.004
TiO_2	-	0.002	0.005	0.003	0.005	0.039	0.043
NiO	-	0.006	0.006	0.001	0.007	0.004	0.011
MnO	-	0.008	0.012	0.002	0.015	0.005	0.000
SiO_2	-	0.012	0.096	0.016	0.016	0.017	0.033
Na_2O	-	0.000	0.019	0.008	0.002	0.001	0.000
MgO	-	0.000	0.000	0.000	0.013	0.001	0.000
CaO	-	0.003	0.001	0.000	0.010	0.003	0.000
K_2O	-	0.004	0.003	0.010	0.011	0.003	0.004
Al_2O_3	-	99.796	98.541	99.524	98.737	97.122	98.029
Total	-	99.904	98.895	99.845	99.396	98.440	99.800

*Cr_2O_3 wt% of sample #1006 was measured by AAS, and the other data were measured by electron microprobe.

Table 2. Relative intensity ratios of R_2 to R_1 at room temperature and atmospheric pressure ($(I_2/I_1)_0$) and the slopes of the wavenumber shifts of R_1 and R_2 with temperature ($d\nu_1/dT$, $d\nu_2/dT$) at atmospheric pressure for ruby samples with different Cr_2O_3 contents.

Sample No.	Cr_2O_3 (wt%)	$(I_2/I_1)_0$	$d\nu_1/dT$ (cm^{-1}/K^{-1})	$d\nu_2/dT$ (cm^{-1}/K^{-1})
1006	0.022	0.856 ± 0.003	-0.1574 ± 0.0011	-0.1561 ± 0.0015
4	0.068	0.678 ± 0.011	-0.1533 ± 0.0010	-0.1542 ± 0.0010
3	0.211	0.620 ± 0.012	-0.1530 ± 0.0008	-0.1541 ± 0.0012
2	0.279	0.626 ± 0.007	-0.1525 ± 0.0007	-0.1543 ± 0.0014
5	0.556	0.651 ± 0.009	-0.1519 ± 0.0008	-0.1522 ± 0.0014
7	1.221	0.611 ± 0.001	-0.1501 ± 0.0012	-0.1494 ± 0.0021
8	1.676	0.748 ± 0.005	-0.1495 ± 0.0011	-0.1560 ± 0.0013

Table 3. Calculated values of the electron-phonon coupling constant a for ruby samples with different contents of Cr_2O_3 (T_D = 760 K, T = 298.15 K).

Sample No.	1006	4	3	2	5	7	8
Cr_2O_3 (wt%)	0.022	0.068	0.211	0.279	0.556	1.221	1.676
a (cm^{-1})	257.2 ± 1.6	250.4 ± 1.5	250.7 ± 1.1	250.7 ± 1.0	248.2 ± 1.1	245.4 ± 1.8	244.3 ± 1.6

Figures

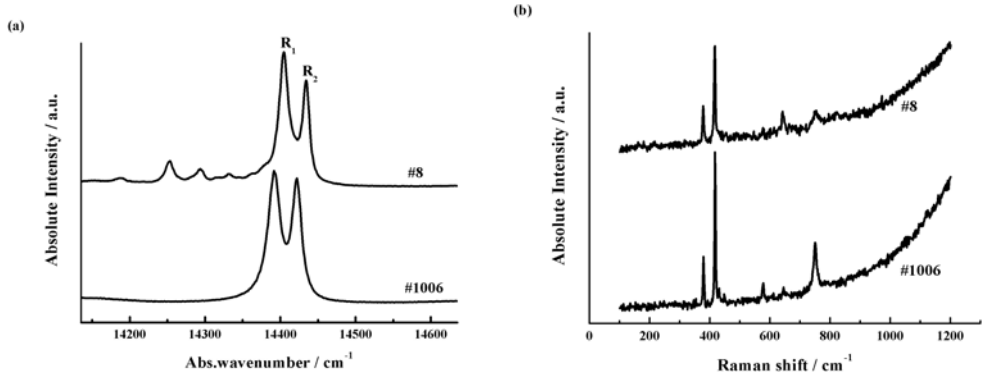

Figure 1

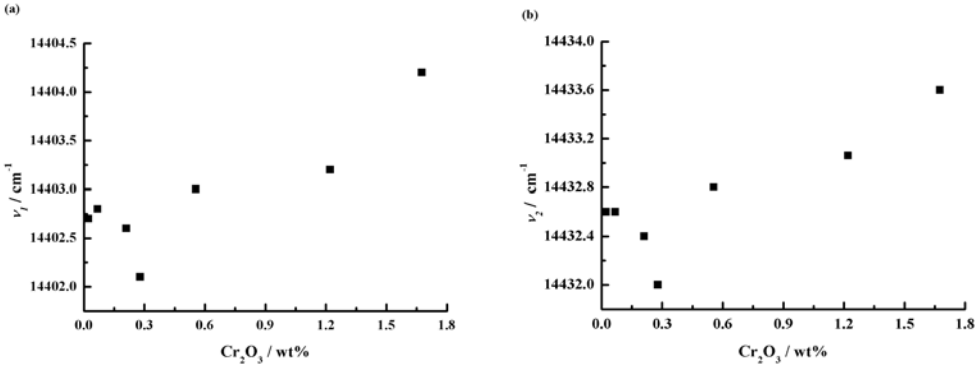

Figure 2

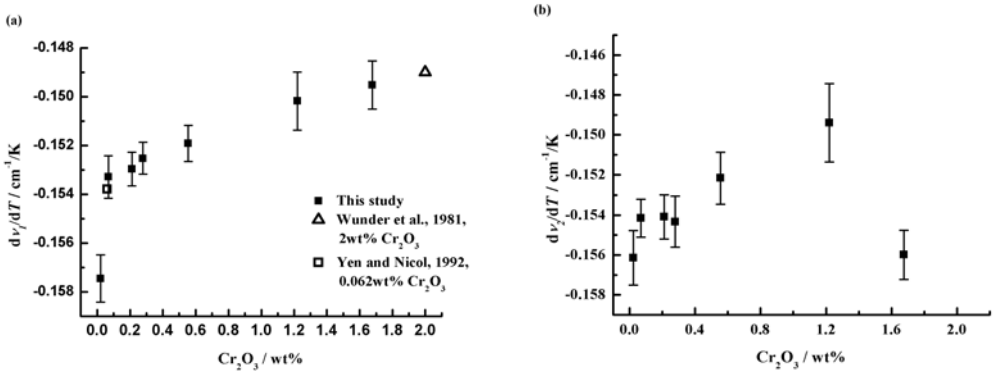

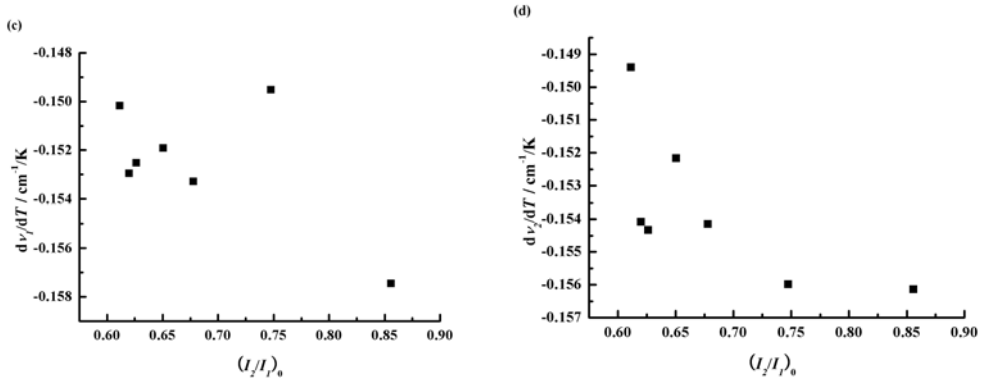

388

389 Figure 3

390

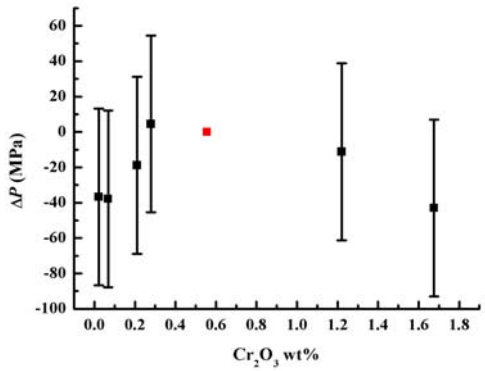

391

392 Figure 4

393

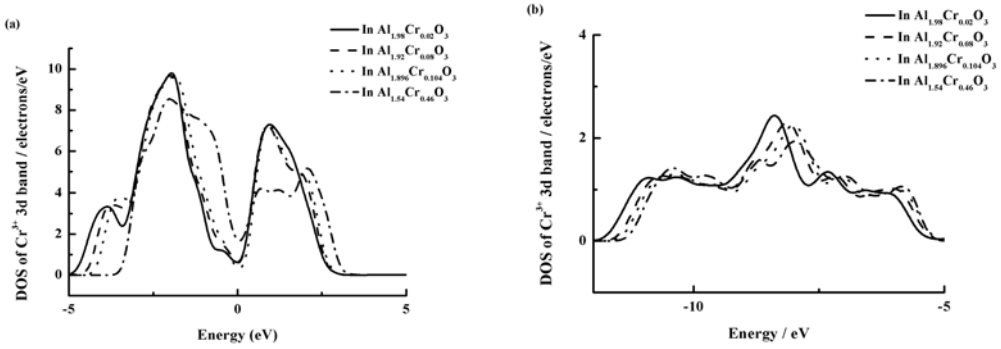

394

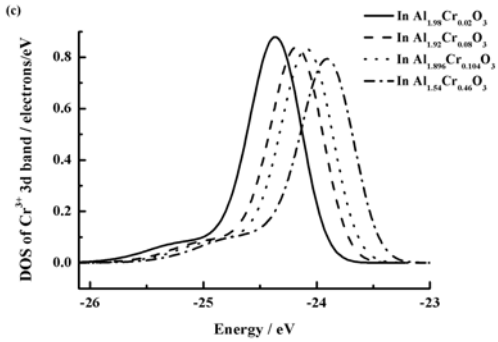

395
396 Figure 5
397

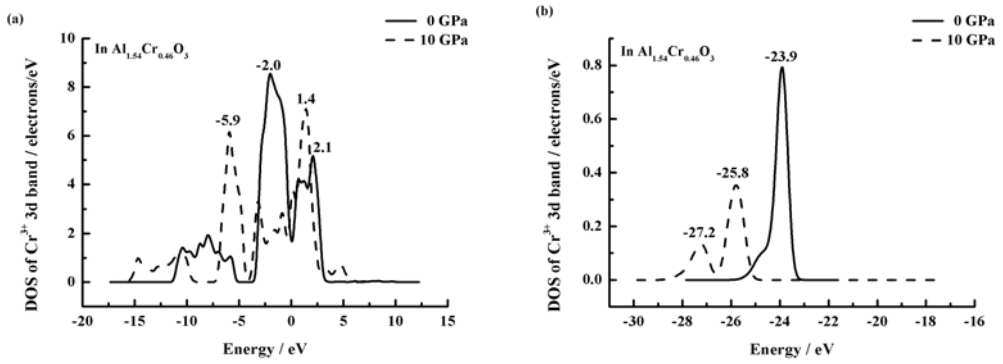

398

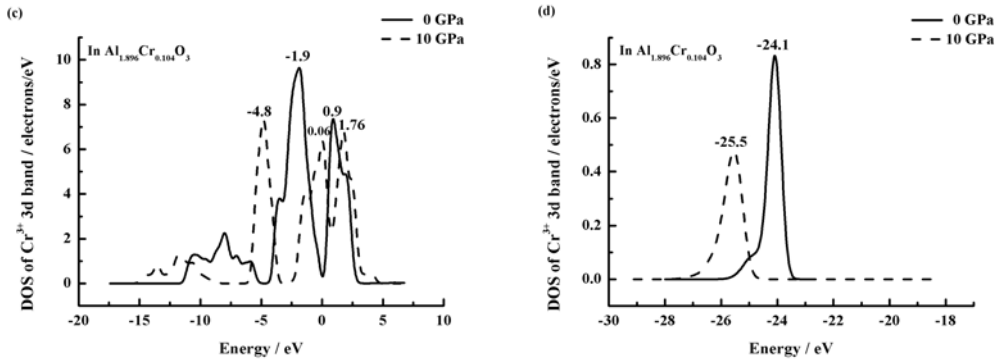

399

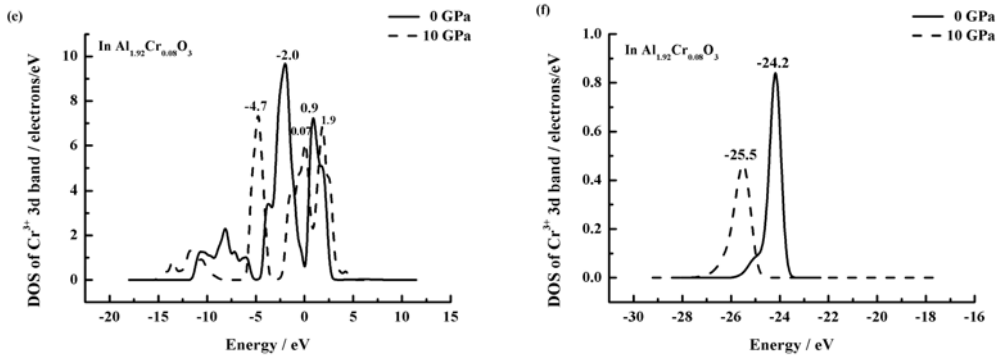

400

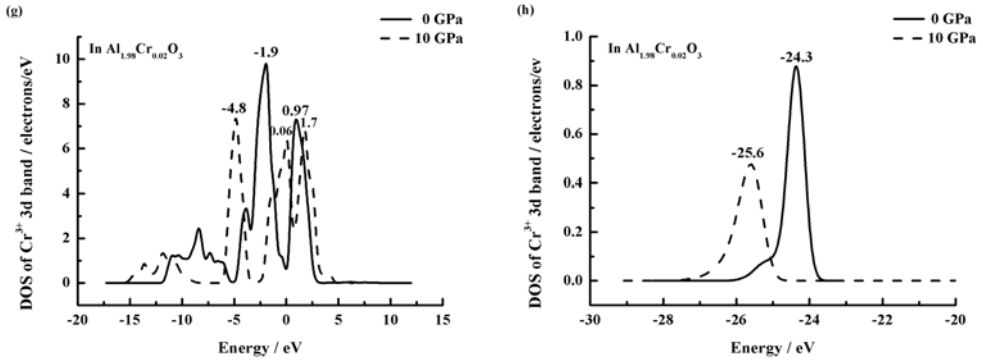

401

402 Figure 6

403

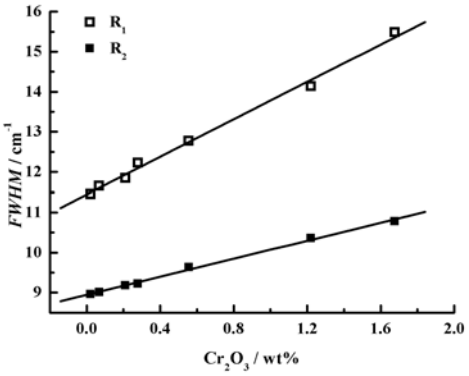

404

405 Figure 7

406

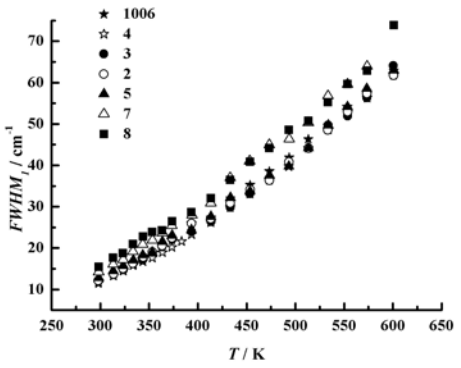

407

408 Figure 8

409

410

Figure captions

Figure 1. (a) Fluorescence spectra of rubies at 298 K and atmospheric pressure, and (b) Raman spectra of rubies at room temperature and atmospheric pressure.

Figure 2. Wavenumber values of R lines at room temperature and atmospheric pressure versus Cr_2O_3 contents in ruby samples, (a) line R_1 and (b) line R_2.

Figure 3. Slopes of the wavenumber shift of (a) line R_1 and (b) line R_2 with temperature at atmospheric pressure versus the Cr_2O_3 contents of different ruby samples, and slopes of the wavenumber shifts of (c) line R_1 and (d) line R_2 with temperature versus the relative intensity ratios of R_2 to R_1 for different ruby samples at room temperature and atmospheric pressure.

Figure 4. Pressure differences between the reference pressure calibrated using ruby sample #5 and those calibrated using the other ruby samples with different Cr_2O_3 contents at 2.0 GPa and room temperature.

Figure 5. Electronic densities of state (DOS) of the Cr^{3+} 3d band in rubies with different Cr_2O_3 contents at room temperature and atmospheric pressure.

Figure 6. Electronic densities of state (DOS) of the Cr^{3+} 3d band in rubies with different Cr_2O_3 contents at room temperature and 10 GPa.

Figure 7. Variations of the full width at half maximum (*FWHM*) of ruby R lines with Cr_2O_3 contents in different ruby samples at atmospheric pressure and room temperature.

Figure 8. Variations of the full width at half maximum of the R_1 line ($FWHM_1$) of different ruby samples at atmospheric pressure and a temperature range of 298-600 K.

Supplement information

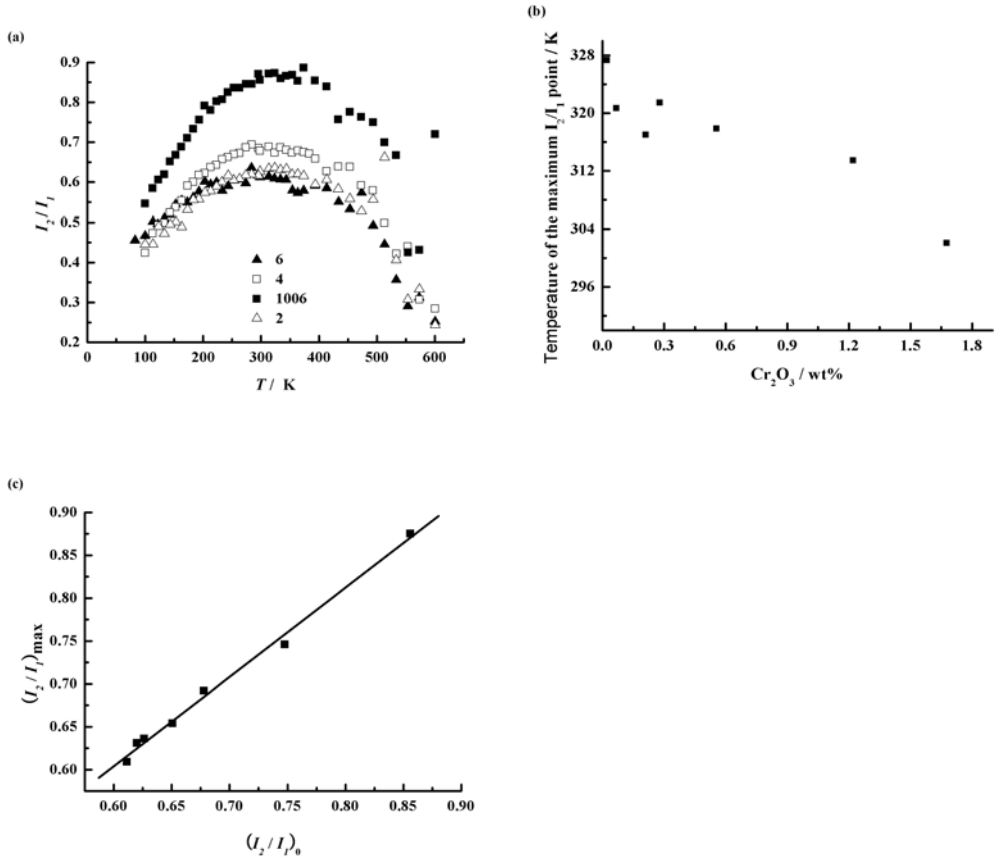

Figure 9. (a) Variations of the relative intensity ratio of R_2 to R_1 (I_2/I_1) at temperatures from 100-600 K at atmospheric pressure for different ruby samples. (b) Plot of the temperatures at which the maximum I_2/I_1 values, $(I_2/I_1)_{max}$ occurred at ambient pressure versus the Cr_2O_3 contents of the ruby samples. (c) Relationship between $(I_2/I_1)_{max}$ at atmospheric pressure and $(I_2/I_1)_0$, the relative intensity ratio of R_2 to R_1 at room temperature and atmospheric pressure, for ruby samples with different Cr_2O_3 contents.